Research Article

Rapid Communications in Mass Spectrometry

Received: 2 October 2016 Revised: 19 December 2016 Accepted: 20 December 2016 Published online in Wiley Online Library

Rapid Commun. Mass Spectrom. **2017**, *31*, 547–560
(wileyonlinelibrary.com) DOI: 10.1002/rcm.7813

Performance of induction module cavity ring-down spectroscopy (IM-CRDS) for measuring $\delta^{18}O$ and $\delta^{2}H$ values of soil, stem, and leaf waters

J. E. Johnson[1,2*], L. Hamann[3], D. L. Dettman[4], D. Kim-Hak[5], S. W. Leavitt[6], R. K. Monson[1,6] and S. A. Papuga[3]

[1]Department of Ecology and Evolutionary Biology, University of Arizona, Tucson, AZ 85721, USA
[2]Department of Global Ecology, Carnegie Institution, 260 Panama Street, Stanford, CA 94305, USA
[3]School of Natural Resources and the Environment, University of Arizona, Tucson, AZ 85721, USA
[4]Department of Geosciences, University of Arizona, Tucson, AZ 85721, USA
[5]Picarro, Inc., 3105 Patrick Henry Drive, Santa Clara, CA 95054, USA
[6]Laboratory of Tree-Ring Research, University of Arizona, Tucson, AZ 85721, USA

RATIONALE: Induction module cavity ring-down spectroscopy (IM-CRDS) has been proposed as a rapid and cost-effective alternative to cryogenic vacuum distillation (CVD) and isotope ratio mass spectrometry (IRMS) for the measurement of $\delta^{18}O$ and $\delta^{2}H$ values in matrix-bound waters. In the current study, we characterized the performance of IM-CRDS relative to CVD and IRMS and investigated the mechanisms responsible for differences between the methods.
METHODS: We collected a set of 75 soil, stem, and leaf water samples, and measured the $\delta^{18}O$ and $\delta^{2}H$ values of each sample with four techniques: CVD and IRMS, CVD and CRDS, CVD and IM-CRDS, and IM-CRDS alone. We then calculated the isotopic errors for each of the three CRDS methods relative to CVD and IRMS, and analyzed the relationships among these errors and suites of diagnostic spectral parameters that are indicative of organic contamination.
RESULTS: The IM-CRDS technique accurately assessed the $\delta^{18}O$ and $\delta^{2}H$ values of pure waters, but exhibited progressively increasing errors for soil waters, stem waters, and leaf waters. For soils, the errors were attributable to subsampling of isotopically heterogeneous source material, whereas for stems and leaves, they were attributable to spectral interference. Unexpectedly, the magnitude of spectral interference was higher for the solid samples analyzed directly via IM-CRDS than for those originally extracted via CVD and then analyzed by IM-CRDS.
CONCLUSIONS: There are many types of matrix-bound water samples for which IM-CRDS measurements include significant errors from spectral interference. As a result, spectral analysis and validation should be incorporated into IM-CRDS post-processing procedures. In the future, IM-CRDS performance could be improved through: (i) identification of the compounds that cause spectral interference, and either (ii) modification of the combustion step to completely oxidize these compounds to CO_2, and/or (iii) incorporation of corrections for these compounds into the spectral fitting models used by the CRDS analyzers.

In the environmental sciences, measurements of the stable isotope composition of oxygen ($\delta^{18}O$ values) and hydrogen ($\delta^{2}H$ values) are routinely performed on liquid water samples extracted from solid matrices. Traditionally, the measurement approach has involved the extraction of waters from solid matrices via cryogenic vacuum distillation (CVD) and subsequent analysis of the distillates via isotope ratio mass spectrometry (IRMS). While the IRMS measurements originally represented the bottleneck in this analysis pathway, improvement in continuous-flow techniques eventually turned the tables,[1] leaving CVD as the rate-limiting step.[2] More recently, the emergence of isotope ratio infrared spectroscopy (IRIS) as a higher-throughput alternative to IRMS has accentuated the long-standing throughput limitations associated with CVD, and highlighted a new set of challenges associated with the organic contaminants that co-extract with water in this technique.[3–7] In combination, these factors have intensified interest in the development of new methods that integrate the extraction step with isotope analysis via IRIS.

To date, two methods have been developed as alternatives to CVD: an induction module (IM) and a microwave extraction chamber. The original version of the IM was designed to extract liquid water into a dry nitrogen stream by induction heating, carry the resulting vapor through a ceramic micropyrolysis column heated to 1200°C to pyrolyze organic contaminants, and pass the cleaned vapor directly into an IRIS analyzer.[8] A revised version of the IM was then designed to combust, rather than pyrolyze, the organic contaminants by replacing the ceramic micropyrolysis column with a metal catalyst heated to only 400°C.[9–11] In a parallel effort, a

* *Correspondence to*: J. E. Johnson, Department of Global Ecology, Carnegie Institution, 260 Panama Street, Stanford, CA 94305, USA.
E-mail: jjohnson@carnegiescience.edu

microwave extraction chamber was designed to extract liquid water into a dry air stream by microwave heating within a sealed vessel, cool the resulting water vapor in a condensation chamber, and carry the cooled vapor directly into an IRIS analyzer.[12] While the initial tests of the IM and microwave extraction chamber have indicated that both techniques have promise, neither has yet been thoroughly characterized relative to CVD and IRMS, and only the IM is currently commercially available.

Three recent studies have evaluated aspects of the performance of the IM. The first two studies examined the micro-combustion module (MCM), the component of the IM that contains the heated catalyst to oxidize volatile organic compounds to CO_2.[9,10] The MCM can be used either within the IM system or downstream of an autosampler and vaporizer system, and these first two studies both used the latter configuration. In tests with natural stem and soil water samples, the MCM was effective at oxidizing low concentrations of methanol, but ineffective at oxidizing high concentrations of ethanol.[9] In tests with artificial mixtures of ethanol, the MCM did not completely oxidize ethanol to CO_2, and instead formed a variety of partial oxidation products.[10] The third study examined the performance of the full IM system (including the MCM) for stem samples, and found that this configuration produced substantial errors relative to CVD and IRMS.[11] The basis of the errors was not clear in this third study because the IM extractions appeared to be complete and there did not appear to be evidence of spectral interference from co-extracted organic compounds.[11]

Here, we report a study of the performance of an IM coupled to an IRIS analyzer for isotopic analysis of soil, stem, and leaf waters. The specific system under evaluation included an IM coupled to a cavity ring-down spectrometer (i.e., induction module cavity ring-down spectroscopy; IM-CRDS). The study objectives were: (i) to quantify the accuracy of IM-CRDS relative to CVD and IRMS, (ii) to diagnose the mechanisms responsible for errors in IM-CRDS relative to CVD and IRMS, and (iii) to determine remedies to correct the errors. To pursue these objectives, we collected a physically and chemically diverse set of soil, stem, and leaf water samples expected to vary in isotopic composition. We measured the $\delta^{18}O$ and $\delta^{2}H$ values of each sample with four techniques (Fig. 1). Building on previous work,[7] we analyzed the relationships between the errors observed for each CRDS method and the suites of spectral parameters that are indicative of organic contamination (Table 1). We then used these relationships to diagnose the types of mechanisms most likely to be responsible for the observed errors (Table 2). The key assumption underlying this approach is that CRDS errors correlated with the diagnostic spectral parameters are likely to be the result of organic contamination, whereas CRDS errors uncorrelated with the spectral parameters are likely to be the result of other mechanisms.

EXPERIMENTAL

Sample collection

We collected 25 different samples each with 3 replicates, for a total of 75 samples. The samples included pure waters ($n = 4 \times 3$), leaf waters ($n = 8 \times 3$), stem waters ($n = 9 \times 3$), and soil waters ($n = 4 \times 3$). The pure waters were of known isotopic composition and were included as check standards, to inspect for fractionations during sample handling and analysis. The soil, stem, and leaf waters were selected to represent a diverse range of soil types and perennial plant species that (i) are of key interest for ecological studies and (ii) exhibit variability in physical and chemical properties that might affect water extraction. The soil samples included a sandy loam and a clay loam with low organic content from the Desert Laboratory on Tumamoc Hill (*ca* 2 km west of downtown Tucson), a silty loam with high organic content from Mt. Bigelow (*ca* 30 km northeast of downtown Tucson in the Santa Catalina Mountains), and a commercially available potting mix, also with high organic content. The plant samples included stems and leaves from *Larrea tridentata*, *Prosopis velutina*, *Acacia constricta*, *Parkinsonia microphylla*, *Fouquieria splendens*, and *Ambrosia deltoidea*, all collected from Tumamoc Hill. Basal and apical succulent stem segments were also included from the cactus species *Opuntia engelmanii* and *Cylindropuntia versicolori* at Tumamoc Hill; for analysis, these samples are grouped with the 'stem' and 'leaf' samples, respectively. In addition, stem samples were included from *Pseudotsuga menziesii*, from Mt. Bigelow. The soil and plant collections were made at midday during summer of 2014 (Jul.-Aug.), fall of 2014 (Oct.-Nov.), spring of 2015 (Mar.-Apr.), and summer of 2015 (Aug.-Sept.). At the field sites, soils, stems, and leaves were collected into 20-mL air-tight glass vials with Polyseal cone-lined screw caps, sealed with Parafilm, and kept on ice. After transfer to the laboratory, the samples were frozen at –4°C until analysis. For analysis, each frozen soil, stem, and leaf sample was divided into two fractions, one for CVD and the other for IM-CRDS.

Cryogenic vacuum distillation

A CVD system was constructed at the Laboratory of Tree-Ring Research, University of Arizona (Tucson, AZ, USA) for this analysis. The extraction system consisted of six distillation units, each comprising a glass sample holder and collection tube, connected to a main vacuum line. For extractions, the main vacuum line was pumped down to a pressure of 10 millitorr with a direct-drive vacuum pump (E2M2, Edwards, Crawley, UK). The vials containing the frozen samples were weighed, uncapped, placed in the sample holders, and attached to the distillation units. The attached sample holders were submerged in liquid nitrogen for 15 min; the distillation units were opened to the main vacuum line for 15 min; and the distillation units were then sealed under vacuum. The pressure was monitored in each distillation unit with vacuum gauges (Convectron Vacuum Measurement System Series 275, Granville-Phillips, Boulder, CO, USA) to ensure that there were no detectable leaks. The sample holders were submerged in deionized water and heated to 100°C by immersion heaters to evaporate the liquid water, while the collection tubes were submerged in liquid nitrogen to condense the resulting water vapor. Each extraction continued until the pressure in the distillation unit returned to the original level, which ranged from a minimum of ~60 min (i.e., for liquid waters) to a maximum of ~3 h (i.e., for soils). The distillates were collected and transferred to a refrigerator. The completeness of the extractions was assessed by weighing the residual solid samples immediately after extraction, transferring them to a

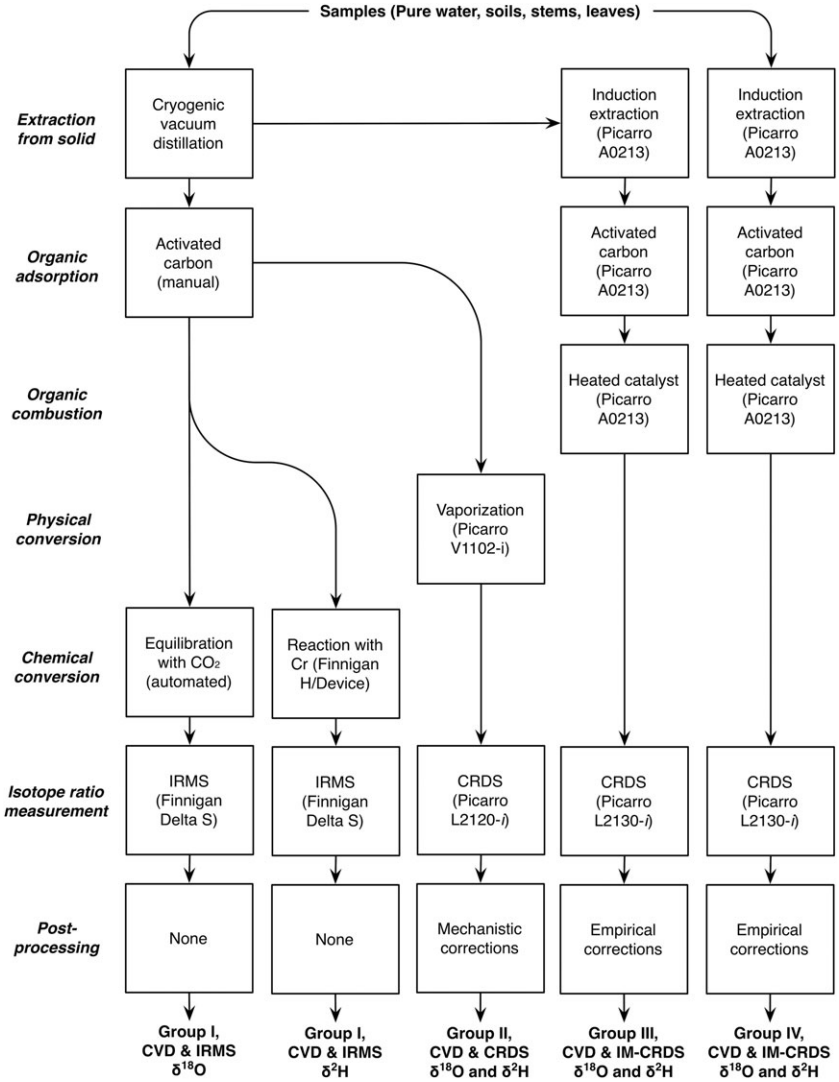

Figure 1. Flow chart of experimental design. In this study, we evaluated the performance of IM-CRDS for analysis of $\delta^{18}O$ and $\delta^{2}H$ values of pure water, soil water, stem water, and leaf water through comparison to several alternative techniques. Abbreviations: IM, induction module; MCM, micro-combustion module; CRDS, cavity ring-down spectroscopy; IRMS, isotope ratio mass spectrometry.

drying oven, holding at 55°C for 72 h, and then re-weighing. Of the 75 samples, 67 were initially extracted with an efficiency >97%. The eight samples with lower initial extraction efficiencies were discarded and the extractions were repeated on new subsets of material from the original collections. Once the extractions were complete, the distilled samples were divided into three fractions, one for IRMS, a second for CRDS, and a third for IM-CRDS (Fig. 1).

Activated carbon treatment

We applied an activated carbon treatment to the distillates that were analyzed by IRMS and regular CRDS. A coarse activated carbon (4–12 mesh) was homogenized to a fine powder with a mortar and pestle to achieve maximum surface area. The homogenized activated carbon was added to each distillate vial in order to achieve a 20% *w*/w slurry. The slurries were incubated for 24 h at 4°C, with periodic vortexing to achieve thorough mixing. After the incubation period, each mixture was filtered through a 0.2-µm syringe-tip filter (54145-U, Sigma Aldrich, St. Louis, MO, USA), transferred to a fresh vial, and sealed with Parafilm. To test for fractionation associated with the activated carbon treatment, subsets from one set of distilled standards were set aside as controls that did not receive the activated carbon treatment, but were otherwise handled identically. Since analysis by IM-CRDS involves on-line treatment with activated carbon, the distillate fraction for IM-CRDS did not receive the manual treatment with activated carbon.

Isotope ratio mass spectrometry (IRMS)

IRMS measurements were made with a Finnigan Delta S isotope ratio mass spectrometer (Thermo Fisher Scientific, West Palm Beach, FL, USA) in the Environmental Isotope

Table 1. Parameters used to diagnose spectral interference. The raw values of these parameters were retrieved from each analyzer's 'Datalog_Private' directory and averaged over the duration of each injection. In both the L2120-*i* and the L2130-*i*, these raw values are inherently sensitive to the water concentration during measurement. However, the introduction of samples to the L2120-*i* via the autosampler and vaporizer produced square pulses of water with little variation in the maximum water concentration, whereas the introduction of samples to the L2130-*i* via the induction module produced shark-fin type pulses of water with a moderate amount of variation in the maximum water concentration. As a result, we corrected only the L2130-*i* measurements for the effects of water concentration, following the method recommended by a recent study[T1]

Instrument	Parameter name	Parameter definition	Diagnostic meaning
L2120-*i*	organic_res	RMS residuals of the least-squares fit (organics)	Indicates how well the observed absorption spectrum can be fit to the spectrum of pure water; poor fit may indicate organic interference
L2120-*i*	organic_shift	Change in constant term of fitted organic baseline	Indicates whether the y-intercept of the baseline underlying the absorption spectrum has been distorted relative to original factory calibration
L2120-*i*	organic_slope	Change in linear term of fitted organic baseline	Indicates whether the slope of the baseline underlying the absorption spectrum has been distorted relative to original factory calibration
L2120-*i*	organic_MeOHampl	Absorption of MeOH peak	Indicates whether methanol (MeOH) is present in the sample, and if present then in what concentration
L2120-*i*	organic_ch4conc	CH_4 mole fraction with no calibration	Indicates whether methane (CH_4) is present in the sample, and if present then in what concentration
L2130-*i*	residuals	RMS residuals of the least-squares fit	Indicates how well the observed absorption spectrum can be fit to the spectrum of pure water; poor fit may indicate organic interference
L2130-*i*	baseline_shift	Change in constant term of fitted baseline	Indicates whether the y-intercept of the baseline underlying the absorption spectrum has been distorted relative to original factory calibration
L2130-i	slope_shift	Change in linear term of fitted baseline	Indicates whether the slope of the baseline underlying the absorption spectrum has been distorted relative to original factory calibration
L2130-i	baseline_curvature	Quadratic term in fitted baseline	Indicates whether any curvature has been introduced into the baseline underlying the absorption spectrum
L2130-i	CH4	Final methane fraction after bottle calibration	Indicates whether methane (CH_4) is present in the sample, and if present then in what concentration

Laboratory, Department of Geosciences, University of Arizona (Tucson, AZ, USA). For oxygen, the samples were equilibrated with CO_2 gas at approximately 15°C in an automated equilibration device coupled to the mass spectrometer. For hydrogen, the samples were reacted at 750°C with Cr metal using a Finnigan H-Device coupled to the mass spectrometer. Standardization was based on distilled water calibration standards referenced to VSMOW2 and SLAP2. Based on repeated measurements of the calibration standards, the analytical precision for these methods was ±0.08‰ for $\delta^{18}O$ values and ±0.9‰ for $\delta^{2}H$ values.

Cavity ring-down spectroscopy (CRDS)

CRDS measurements were made with a L2120-*i* cavity ring-down spectrometer equipped with a V1102-i high-precision vaporizer (Picarro, Inc., Santa Clara, CA, USA) and a HTC PAL autosampler (Leap Technologies, Carrboro, NC, USA). The L2120-*i* measures three of the major isotopologues of water based on absorption at three near-infrared absorption lines close to 7184 cm^{-1} (1392 nm). The specific lines that are utilized are 7183.685 cm^{-1} (1392.043 nm) for $^{1}H^{1}H^{16}O$, 7183.585 cm^{-1} (1392.063 nm) for $^{1}H^{1}H^{18}O$, and 7183.972 cm^{-1} (1391.988 nm) for $^{1}H^{2}H^{16}O$.[13–15] All the measurements were performed in the air carrier mode, with air provided from a cylinder of ultra-high-purity compressed air (<1 ppm H_2O, <0.01 ppm total hydrogen content, <0.01 ppm CO, <0.001 ppm NO_x, <0.001 ppm SO_2; Ultrapure Air, Scott-Marrin, Inc., Riverside, CA, USA). For analyses, 1.5-mL aliquots of each sample were pipetted into 1.8-mL glass vials with polypropylene screw caps and bonded PTFE-silicone septa (66020-950 and 46610-700; VWR, Radnor, PA, USA). The autosampler sampled the vials and injected the samples into the vaporizer on a 9-min cycle, using a 10-µL syringe (SGE 10R-C/T-5/0.47C; Trajan Scientific Americas, Inc., Austin, TX, USA), which was rinsed twice in *N*-methyl-2-pyrrolidone (99.5%, Acros Organics, Fisher Scientific, Pittsburgh, PA, USA) before each injection. The vaporizer was run at 110°C; the vaporizer septum was replaced every 250 injections; and each sample was injected 10 times. To remove memory effects from the resulting dataset, we discarded the initial seven injections from each sample and retained the final three injections for statistical analyses. As with the IRMS measurements, standardization was based on distilled water calibration standards referenced to VSMOW2

Rapid Communications in Mass Spectrometry

Table 2. Classes of mechanisms potentially responsible for CRDS errors. Classes 1–3 describe processes that result in the analysis of pure water samples that do not have the same stable isotopic composition as the water in the original samples (i.e., 'non-spectral error mechanisms'). Classes 4–6 describe processes that result in the analysis of mixtures of water and trace organic contaminants that are spectrally active in the regions targeted by the L2120-*i* and L2130-*i* analyzers (i.e., 'spectral error mechanisms')

Class	Mechanism	Evidence for mechanism
1	Differences in physical subsampling of solid material	In any CRDS analysis, isotopic errors are uncorrelated to spectral indices, and are distributed around a mean value of zero
2	Incomplete extraction of liquid water from solid matrix	In any CRDS analysis, isotopic errors are uncorrelated to spectral indices, and are preferentially distributed around a negative mean value
3	Contributions from water vapor formed during organic oxidation	In CRDS alone, isotopic errors correlated to spectral indices; in IM-CRDS solid or liquid analysis, isotopic errors uncorrelated to spectral indices, and larger for $\delta^{18}O$ values than for $\delta^{2}H$ values
4	Interference from compounds that are co-extracted during cryogenic distillation, but can be oxidized	In CRDS alone, isotopic errors are large and correlated to spectral indices; in IM-CRDS solid and liquid analysis, errors are reduced or absent
5	Interference from compounds that are the products of oxidation reactions in the micro-combustion module	In IM-CRDS solid or liquid analysis, isotopic errors are correlated to spectral indices; in CRDS alone, isotopic errors are uncorrelated to spectral indices
6	Interference from compounds that are not co-extracted during cryogenic distillation, but are during induction extraction	In IM-CRDS solid analysis, isotopic errors are correlated to spectral indices; in IM-CRDS liquid analysis, isotopic errors are uncorrelated to spectral indices

and SLAP2. Based on repeated measurements of the calibration standards, the analytical precision for this method was ±0.20‰ for $\delta^{18}O$ values and ±0.7‰ for $\delta^{2}H$ values.

Induction module cavity ring-down spectroscopy (IM-CRDS)

IM-CRDS measurements were made with a L2130-*i* cavity ring-down spectrometer equipped with an A0213 induction module (Picarro, Inc.). The L2130-*i* measures three of the major isotopologues of water based on absorption at three near-infrared absorption lines close to 7200 cm^{-1} (1389 nm). The specific lines that are utilized are 7200.133 cm^{-1} (1388.863 nm) for $^{1}H^{1}H^{16}O$, 7199.961 cm^{-1} (1388.896 nm) for $^{1}H^{1}H^{18}O$, and 7200.302 cm^{-1} (1388.831 nm) for $^{1}H^{2}H^{16}O$.[13–15] All of the measurements were performed in the air carrier mode, with air provided from a cylinder of ultra-zero compressed air (<3 ppm H_2O, <0.1 ppm total hydrogen content, <1 ppm CO, <1 ppm CO_2; ALPHAGAZ1, Air Liquide, Houston, TX, USA). Samples were prepared for measurement in three ways: (i) liquid samples were injected onto a glass-fiber filter paper disc and placed into a metal clip; (ii) leaf and stem samples were placed directly into a metal clip; (iii) soil samples were placed into a metallic cylinder and sealed off with metal wool. Since each sample could only contain 3–10 µL of water, there was a greater risk of evaporative enrichment during preparation for the IM extractions than for the CVD extractions. As a result, samples were not weighed prior to IM extraction as they were prior to CVD extraction. Instead, each prepared sample was quickly placed into a glass vial, sealed with a septum, and loaded into the IM.

To ensure that the extractions would be complete for the different types of samples, we selected values of the manufacturer's parameters 'heatTime', 'polyA', 'polyB', and 'polyC' that allowed each pulse of extracted water vapor to decay back down to the background level before the end of an analysis cycle (Fig. 2). To ensure that the differences in the extraction methods did not introduce isotopic artifacts, we analyzed one set of check standards on each extraction method. To address issues related to sample memory, we performed replicate analyses of each individual sample until the apparent $\delta^{18}O$ and $\delta^{2}H$ values stabilized. We determined

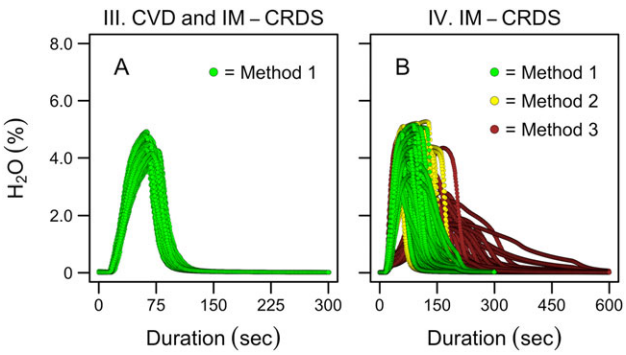

Figure 2. Induction module extraction methods. Water concentrations are plotted as a function of time for all analytical replicates of the samples measured via CVD and IM-CRDS (A) and IM-CRDS alone (B). For the samples initially extracted via CVD, all the IM extractions were performed with Method 1. For the solid samples, Method 1 was applied to leaves, Method 2 to stems, and Method 3 to soils. For Method 1, heatTime =180 sec, polyA =0.00021, polyB =0.00001, and polyC =13; for Method 2, heatTime =180 s, polyA =0.00003, polyB =0.03, and polyC =15; and for Method 3, heatTime =480 sec, polyA =0.00003, polyB =0.4, and polyC =25. [Color figure can be viewed at wileyonlinelibrary.com]

stability with two criteria: (i) standard deviation of three sequential replicates ≤0.75‰ for $\delta^{18}O$ values and ≤2.5‰ for $\delta^{2}H$ values and (ii) mean values of those replicates fluctuating around asymptotes for both $\delta^{18}O$ and $\delta^{2}H$ values. On average, seven replicate analyses were required to satisfy these criteria. In the resulting dataset, we discarded all the initial injections, and retained the final three injections from each sample for statistical analyses. As with the other types of measurements, standardization was based on distilled water calibration standards referenced to VSMOW2 and SLAP2. Based on repeated measurements of the calibration standards, the analytical precision for the leaf, stem, and soil methods was ±0.15, 0.18, and 0.20‰ for $\delta^{18}O$ values and ±1.2, 1.4, and 1.0‰ for $\delta^{2}H$ values, respectively.

Data analysis

Notation

The isotope ratios were expressed relative to the international standard VSMOW (Vienna Standard Mean Ocean Water):

$$\delta^{18}O \text{ or } \delta^{2}H\ (‰) = \left(R_{sample}/R_{VSMOW} - 1\right) \quad (1)$$

where R_{sample} and R_{VSMOW} represent the ratios of the abundance of the heavy and light isotopologues in the samples and international standard, respectively (i.e., $^{1}H^{1}H^{18}O/^{1}H^{1}H^{16}O$ and $^{1}H^{2}H^{16}O/^{1}H^{1}H^{16}O$). The raw $\delta^{18}O$ and $\delta^{2}H$ values were standardized based on the calibration standards that were analyzed concurrently with the samples. While different calibration standards were used for each of the three instruments, each set of standards bracketed the isotope ratios of the unknowns and was used to generate a first-order linear model relating the raw isotope ratios to the true values.

Effects of CVD and manual activated carbon treatment

We compared the true isotopic compositions of the standards (i.e., obtained by IRMS before the distillations) with the isotopic compositions that were obtained by IRMS after the distillations and activated carbon treatments (i.e., n = 12 samples). To determine the basis of any differences, we also compared a subset of the standards that did and did not receive the activated carbon treatment (i.e., n = 4 samples).

Similarities and differences between CRDS and IRMS

We used linear mixed-effects models to characterize differences between the CRDS and IRMS values while accounting for the effects of sample type. All analyses were performed in R.[16] For each combination of predictor and response variables, we fitted a mixed-effects model using the 'lmer()' function from the package 'lme4'.[17] Each model included (i) the IRMS measurement as the response variable, (ii) one of the CRDS measurements as the fixed effect predictor (with intercept and slope), and (iii) the sample type as the random effect predictor (with intercept only). We assessed the significance of each predictor using the package 'lmerTest'.[18] Models where the random effect predictor was not significant were re-fitted with the fixed effect only using the function 'lm()' in base R. The overall model fit was then summarized with: (i) P-values for individual fixed and random effects, (ii) the root mean square error (RMSE), and (iii) the marginal (i.e., fixed effect only) or conditional (i.e., fixed and random effect) R^2.[19]

Mechanisms underlying CRDS and IRMS differences

We calculated the differences between the $\delta^{18}O$ and $\delta^{2}H$ values determined by IRMS versus those by each of the three CRDS methods as: $\Delta\delta^{18}O = \delta^{18}O_{CRDS} - \delta^{18}O_{IRMS}$ and $\Delta\delta^{2}H = \delta^{2}H_{CRDS} - \delta^{2}H_{IRMS}$. For convenience, we will refer to $\Delta\delta^{18}O$ and $\Delta\delta^{2}H$ as 'isotopic error terms'. We then used mixed-effects models to identify the spectral parameters that were the best predictors of the isotopic error terms (Table 1). The model analysis procedure was analogous to that described in the previous section, with the following exception: each model included (i) one of the isotopic error terms as the response variable, (ii) a spectral parameter as the fixed effect predictor (with intercept and slope), and (iii) the sample type as the random effect predictor (with intercept only). This allowed us to consider five alternative models to explain each isotopic error term (i.e., one model per spectral parameter per instrument). We used these models to diagnose the types of mechanisms most likely to be responsible for the observed errors in each method (Table 2).

Approaches for resolving CRDS and IRMS differences

For the L2120-*i* measurements, we calculated organic-corrected $\delta^{18}O$ and $\delta^{2}H$ values as described by the manufacturer and as recommended by a previous study.[9] Briefly, we retrieved the organic-filtered amplitudes of the $^{1}H^{1}H^{18}O$, $^{1}H^{1}H^{16}O$, and $^{1}H^{2}H^{16}O$ peaks from the analyzer's 'Datalog_Private' directory (organic_77, organic_splinemax, organic_82, respectively) and the instrument-specific intercept and slope from the analyzer's 'InstrCal_Air.ini' script. We then calculated organic-corrected $\delta^{18}O$ and $\delta^{2}H$ values as:

$$Y = X \cdot \beta + \varepsilon \quad (2)$$

where Y represents a vector of corrected (but uncalibrated) $\delta^{18}O$ or $\delta^{2}H$ values, X represents a vector of the fixed effect predictors (ratio of organic_77/organic_splinemax or organic_82/organic_splinemax), β represents a vector of regression coefficients (the instrument-specific intercept and slope), and ε represents a vector of random errors. The organic-corrected values were then calibrated to the isotope standards with the same approach originally applied to the organic-uncorrected values.

In the L2130-*i*, organic-filtered amplitudes of the $^{1}H^{1}H^{18}O$, $^{1}H^{1}H^{16}O$, and $^{1}H^{2}H^{16}O$ peaks are not reported as they are reported for the L2120-*i*. As a result, organic-corrected $\delta^{18}O$ and $\delta^{2}H$ values cannot be calculated for the L2130-*i* using the mechanistic model that applies to the L2120-*i*. Instead, we calculated isotopic corrections based on the empirical models that we developed relating the spectral parameter 'residuals' to the $\Delta\delta^{18}O$ and $\Delta\delta^{2}H$ values:

$$Y_{correction} = X \cdot \beta + Z \cdot u + \varepsilon \quad (3)$$

where $Y_{correction}$ represents a vector of isotopic corrections for $\delta^{18}O$ or $\delta^{2}H$ values, X represents a vector of fixed effect predictors (the 'residuals' parameter), Z represents a vector

of random effect predictors (sample type), β represents a vector of fixed effect coefficients, u represents a vector of random effect coefficients, and ε represents a vector of random errors. We then applied the corrections as:

$$Y = Y_{raw} - Y_{correction} \quad (4)$$

where Y_{raw} represents the raw $\delta^{18}O$ or $\delta^{2}H$ values and Y represents the organic-corrected $\delta^{18}O$ or $\delta^{2}H$ values. Since these models utilize regression coefficients determined from the sample set, we use them only to illustrate the degree to which the accuracy and precision of the IM-CRDS measurements could improve if the observed spectral interference were corrected.

RESULTS

Effects of CVD and manual activated carbon treatment

For the pure water check standards, the $\delta^{18}O$ and $\delta^{2}H$ values were slightly higher than the original true values after CVD and manual activated carbon treatment (n = 12; for $\Delta\delta^{18}O$, 0.19 ± 0.26‰; for $\Delta\delta^{2}H$, 0.2 ± 1.8‰). The increase was statistically significant for the $\delta^{18}O$ values (P_{fixed} = 0.026), but not for the $\delta^{2}H$ values ($P_{fixed} > 0.050$). For the check standards, the differences in the $\delta^{18}O$ and $\delta^{2}H$ values before and after activated carbon treatment alone were not statistically significant (n = 4; $P_{fixed} > 0.050$). Since all these errors fell either within or very close to the precision of the IRMS method, no statistical corrections were applied to the samples for the effects of CVD or manual activated carbon treatment. The data are available as Supporting Information.

Similarities and differences between CRDS and IRMS

Across the three CRDS methods, there was significant agreement between the CRDS and IRMS values (Fig. 3; $P_{fixed} < 0.001$ for each comparison). In general, agreement between the various techniques was highest for pure waters, and decreased progressively for soil waters, stem waters, and leaf waters. For all three sample types, the L2120-*i* analyses of distillates tended to underestimate the true values of $\delta^{18}O$ and $\delta^{2}H$ (Figs. 3(A) and 3(D)), whereas the L2130-*i* analyses of both distillates and solids tended to overestimate the true values (Figs. 3(B) and 3(C), and 3(E) and 3(F)). Sample type had a significant effect on the relationship between the CVD and CRDS measurements and the CVD and IRMS measurements (Figs. 3(A) and 3(D); $P_{random} < 0.001$ for $\delta^{18}O$ and $\delta^{2}H$ values), but did not have a significant effect on the relationship between the IM-CRDS measurements and the CVD and IRMS measurements (Figs. 3(C) and 3(F); $P_{random} > 0.050$ for $\delta^{18}O$ and $\delta^{2}H$ values). For the CVD and IM-CRDS measurements, the sample type effect was not significant for $\delta^{18}O$ values (Fig. 3(B); $P_{random} > 0.050$), and was only marginally significant for $\delta^{2}H$ values (Fig. 3(E); P_{random} = 0.040).

Mechanisms underlying CRDS and IRMS differences

For the CVD and CRDS measurements, $\Delta\delta^{18}O$ and $\Delta\delta^{2}H$ were completely unrelated to 'organic_res', 'organic_shift', and 'organic_slope' for all the sample types (Figs. 4(A)–4(C) and 4(F)–4(H); $P_{fixed} > 0.050$ for all). The 'ch4_ppm' parameter was a significant predictor of $\Delta\delta^{18}O$ and $\Delta\delta^{2}H$, but explained relatively little of the variation in these terms (Figs. 4(E) and 4(J); P_{fixed} and $P_{random} < 0.001$ for both). In contrast,

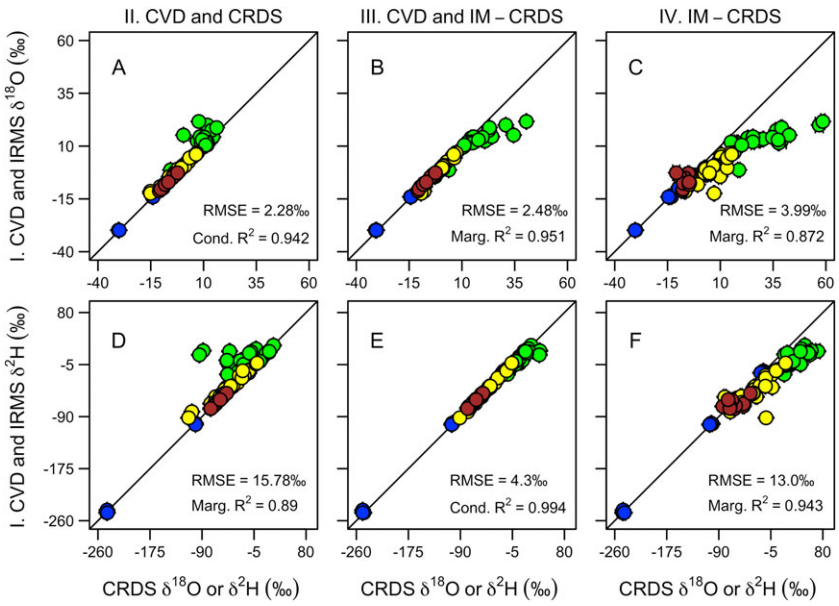

Figure 3. Overall differences in $\delta^{18}O$ and $\delta^{2}H$ values between CRDS and IRMS measurements. Points indicate means ± standard deviation for pure waters (blue; n = 12), leaf waters (green; n = 24), stem waters (yellow; n = 27), and soil waters (brown; n = 12) in each of the three treatment groups (II, III, IV; as defined in Fig. 1). [Color figure can be viewed at wileyonlinelibrary.com]

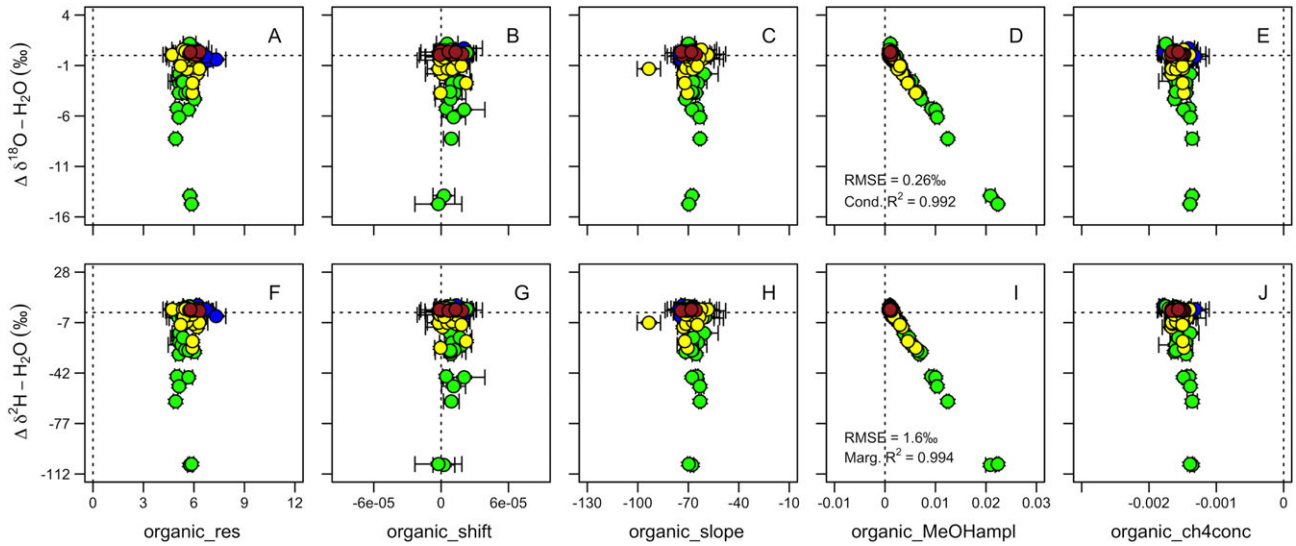

Figure 4. Mechanisms driving differences in $\delta^{18}O$ and $\delta^{2}H$ values between CVD and CRDS versus CVD and IRMS measurements. Isotopic errors are plotted as a function of the raw (non-normalized) spectral indices. Points indicate means ± standard deviation for individual samples of pure waters (blue; n = 12), leaf waters (green; n = 24), stem waters (yellow; n = 27), and soil waters (brown; n = 12) in treatment group II (i.e., liquid distillates analyzed with L2120-*i* without induction module; Fig. 1). Dashed lines indicate the zero positions on each axis. [Color figure can be viewed at wileyonlinelibrary.com]

'organic_MeOHampl' was a significant predictor of $\Delta\delta^{18}O$ and $\Delta\delta^{2}H$ and explained the majority of the variation in these terms (Figs. 4(D) and 4(I); $P_{fixed} < 0.001$ for both). For $\Delta\delta^{18}O$, these relationships differed slightly between sample types (Fig. 4(D); $P_{random} = 0.005$), but, for $\Delta\delta^{2}H$, there were no differences between sample types (Fig. 4(I); $P_{random} > 0.100$).

For the CVD and IM-CRDS measurements, both isotopic error terms had significant linear relationships with 'residuals', 'slope_shift', 'baseline_curvature', and 'ch4_ppm' (Figs. 5(A), 5(C)–5(F), 5(H)–5(J); $P_{fixed} < 0.001$ for all). A similar trend was evident with 'baseline_shift', but several outliers weakened the overall relationship (Figs. 5(B) and 5(G); $P_{fixed} = 0.093$ and 0.045, respectively). The samples with large isotopic error terms also had positive values of 'residuals', 'baseline_shift', and 'baseline_curvature', but negative values of 'slope_shift' and 'ch4_ppm' (Figs. 5(A)–5(J)). The stem samples from *Pseudotsuga menziesii* departed from the general pattern to a large degree in 'baseline_shift', and to a lesser degree in 'slope_shift' and 'baseline_curvature' (Figs. 5(B)–5(D), 5(G)–5(I)). Overall, the models based on 'residuals' accounted for the largest fractions of the variation in the isotopic error terms (Figs. 5(A) and 5(F)). For both $\Delta\delta^{18}O$ and

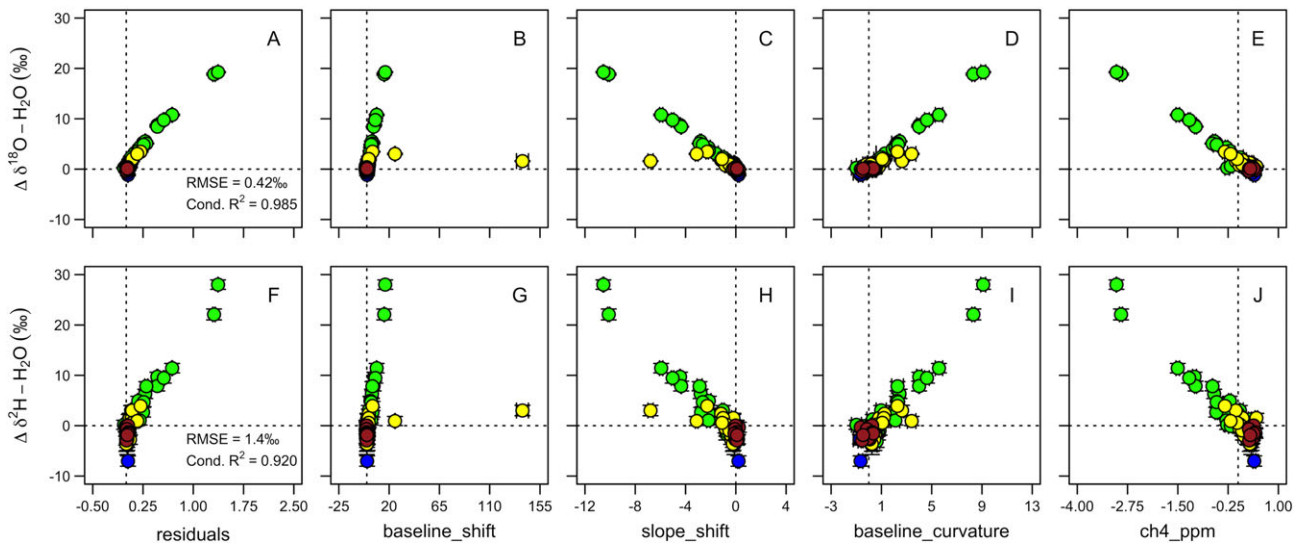

Figure 5. Mechanisms driving differences in $\delta^{18}O$ and $\delta^{2}H$ values between CVD and IM-CRDS versus CVD and IRMS. Isotopic errors are plotted as a function of normalized spectral indices. Points indicate means ± standard deviation for individual samples of pure waters (blue; n = 12), leaf waters (green; n = 24), stem waters (yellow; n = 27), and soil waters (brown; n = 12) in treatment group III (i.e., liquid distillates analyzed with L2130-*i* with induction module; Fig. 1). Dashed lines indicate the zero positions on each axis. [Color figure can be viewed at wileyonlinelibrary.com]

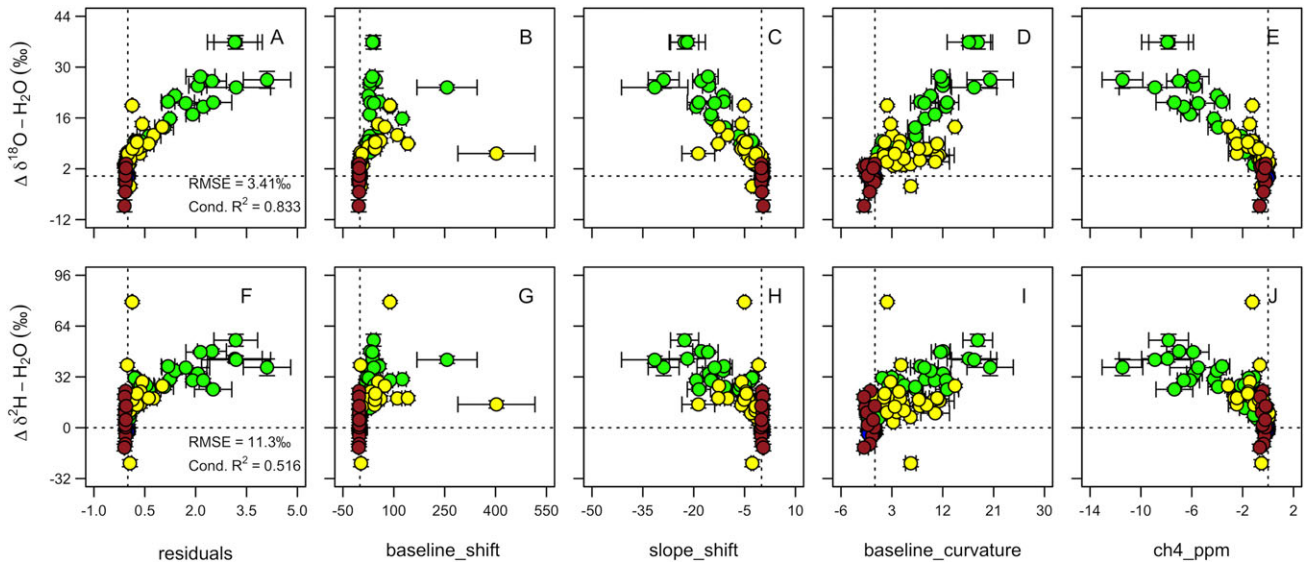

Figure 6. Mechanisms driving differences in $\delta^{18}O$ and $\delta^{2}H$ values between IM-CRDS versus CVD and IRMS. Isotopic errors are plotted as a function of normalized spectral indices. Points indicate means ± standard deviation for individual samples of pure waters (blue; $n = 12$), leaf waters (green; $n = 24$), stem waters (yellow; $n = 27$), and soil waters (brown; $n = 12$) in treatment group IV (i.e., solid samples analyzed with L2130-*i* with induction module; Fig. 1). Dashed lines indicate the zero positions on each axis. [Color figure can be viewed at wileyonlinelibrary.com]

$\Delta\delta^{2}H$, the relationships with 'residuals' differed significantly between sample types (Figs. 5(A) and 5(F); $P_{random} < 0.001$ and $P = 0.008$, respectively).

For the IM-CRDS measurements, the relationships between the isotopic error terms and the diagnostic spectral parameters were similar to those in the CVD and IM-CRDS measurements, but with more noise and stronger differences between sample types (Fig. 6). Both isotopic error terms had significant linear relationships with all the spectral parameters (Figs. 6(A)–6(J); for $\Delta\delta^{18}O$ and $\Delta\delta^{2}H$, $P_{fixed} < 0.001$ for 'residuals', 'slope_shift', 'ch4_ppm'; $P_{fixed} < 0.01$ for 'baseline_curvature'; $P_{fixed} < 0.05$ for 'baseline_shift'). The samples with large positive isotopic error terms also had positive values of 'residuals', 'baseline_shift', and 'baseline_curvature', but negative values of 'slope_shift' and 'ch4_ppm' (Figs. 6(A)–6(J)). Sample type was a significant random effect in nine of the ten models (i.e., $P > 0.050$ only for the relationship between $\Delta\delta^{2}H$ and 'baseline_shift'). The sample types that had the largest isotopic error terms and/or largest deviations from the pure water spectral parameters were leaves and stems from *Pseudotsuga menziesii*, *Ambrosia deltoidea*, and *Opuntia engelmanii*. Overall, the models based on 'residuals' again accounted for the largest fractions of the variation in the isotopic error terms (Figs. 6(A) and 6(F)).

Mechanisms underlying differences among the three CRDS methods

The 'organic_MeOHampl' parameter from CVD and CRDS was strongly and positively linearly correlated to the 'residuals' parameter from CVD and IM-CRDS (Fig. 7(A); $P_{fixed} < 0.001$). The relationship between the two spectral parameters varied slightly between sample types, with intercepts highest for pure water and decreasing for soil water, stem water, and leaf water ($P_{random} = 0.008$). Taking these effects into account, variation in 'organic_MeOHampl' from

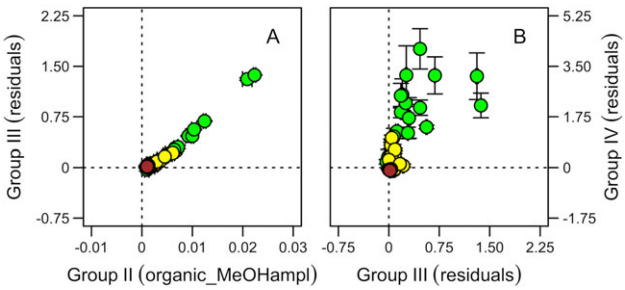

Figure 7. Mechanisms driving differences in $\delta^{18}O$ and $\delta^{2}H$ values among the three CRDS methods. For each sample, plots compare the values of the spectral parameters that best predicted isotopic errors in each type of CRDS analysis. Points indicate means ± standard deviation for individual samples of pure waters ($n = 12$), leaf waters ($n = 24$), stem waters ($n = 27$), and soil waters ($n = 12$). [Color figure can be viewed at wileyonlinelibrary.com]

CVD and CRDS explained nearly all the variation in 'residuals' from CVD and IM-CRDS (conditional $R^2 = 0.982$). In comparison, 'residuals' from CVD and IM-CRDS was only weakly correlated with 'residuals' from IM-CRDS (Fig. 7(B); $P_{fixed} < 0.001$). The relationship between the two spectral parameters varied between sample types, with intercepts lowest for soil water and increasing for pure water, stem water, and leaf water ($P_{random} < 0.001$). Taking these effects into account, variation in 'residuals' from CVD and IM-CRDS explained approximately half the variation in 'residuals' from IM-CRDS (conditional $R^2 = 0.585$).

Approaches for resolving CRDS and IRMS differences

Within the CVD and CRDS measurements, the post-processing correction based on the organic-filtered amplitudes of the $^{1}H^{1}H^{18}O$, $^{1}H^{1}H^{16}O$, and $^{1}H^{2}H^{16}O$ peaks

brought the corrected CRDS values into good agreement with the corresponding IRMS values (Figs. 8(A) and 8(D); $P_{fixed} < 0.001$). There were no effects of sample type on these relationships ($P_{random} > 0.050$). Within the CVD and IM-CRDS measurements, the post-processing correction based on 'residuals' also brought the corrected CRDS values into good agreement with the corresponding IRMS values (Fig. 8(B) and 8(E); $P_{fixed} < 0.001$). There were also no effects of sample type on these relationships ($P_{random} > 0.050$). Within the IM-CRDS measurements, the post-processing correction based on 'residuals' brought the corrected CRDS values into closer agreement with the corresponding IRMS values (Figs. 8(C) and 8(F); $P_{fixed} < 0.001$). Sample type still had a marginal effect on the relationships for $\delta^{18}O$ values ($P_{random} = 0.070$), but no effect for $\delta^{2}H$ values ($P_{random} > 0.050$).

DISCUSSION

Accuracy of CRDS methods relative to cryogenic vacuum distillation and IRMS

All three CRDS methods performed satisfactorily for the pure water check standards, as expected from previous measurements with the L2120-*i* with vaporizer, the L2120-*i* with MCM,[9] the L2120-*i* with an IM,[11] and the L2130-*i* with an MCM.[10] For the soil distillates, the L2120-*i* with vaporizer and the L2130-*i* with an IM produced consistent results with relatively minor errors that were within the lower end of the range of errors previously reported for soil distillates.[4,6,7,9,20] For the solid soil samples, the errors from the L2130-*i* with an IM were distributed around a mean of approximately zero, but extended across a substantially wider range than was observed for the soil distillates. There were no previous measurements of solid soils analyzed with the IM available for comparison. For the stem and leaf distillates, the mean errors associated with the L2120-*i* with vaporizer and the L2130-*i* with an IM were much greater than those for the soil distillates, and the largest errors were within the upper end of the range of previous reports.[4,6,7,9,20] For the solid stem and leaf samples, the magnitude of the errors from the L2130-*i* with the IM varied substantially between species, and the largest errors were approximately four times greater than those previously reported for *Artemisia tridentata* stems analyzed with the L2120-*i* with the IM.[11]

Mechanisms responsible for errors in CRDS methods

The vast majority of the errors in all three CRDS methods appear to be attributable to spectral interference (i.e., mechanisms within classes 4–6 in Table 2). However, a small component of the errors in IM-CRDS also appears to be attributable to non-spectral mechanisms (i.e., within classes 1–3 in Table 2). Below, we discuss the evidence for attribution of the isotopic errors to the spectral and non-spectral mechanisms.

Spectral mechanisms

The first line of evidence that spectral interference is responsible for the major component of the CRDS errors is the variation in mathematical sign of the isotopic errors: negative in the set of CVD and CRDS measurements, but positive in both sets of IM-CRDS measurements (Fig. 3). The tendency for errors in the L2120-*i* measurements to be negative

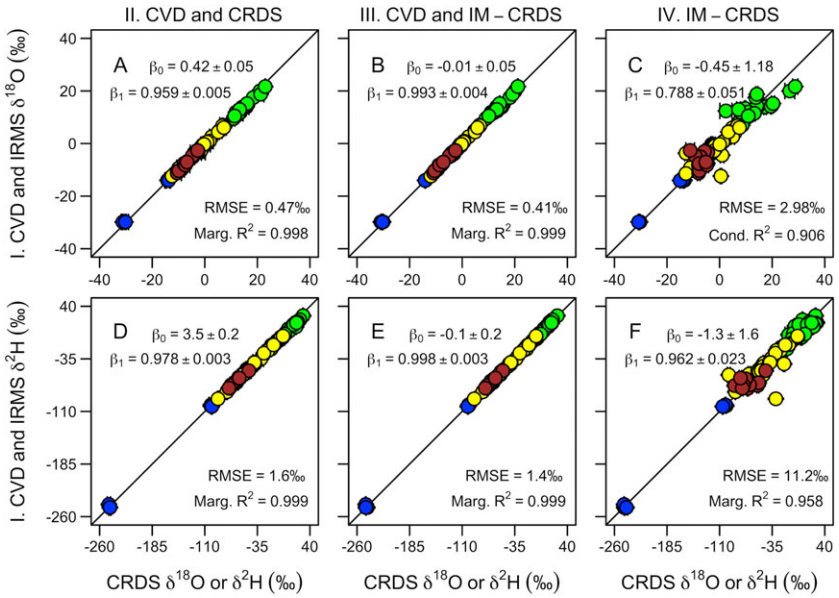

Figure 8. Approaches for correcting differences in $\delta^{18}O$ and $\delta^{2}H$ values between CRDS and IRMS. Points indicate means ± standard deviation for individual samples of pure waters (n = 12), leaf waters (n = 24), stem waters (n = 27), and soil waters (n = 12) in each of the three treatment groups (II, III, IV; as defined in Fig. 1). Solid lines indicate the 1:1 relationship between corrected CRDS measurements versus IRMS measurements. [Color figure can be viewed at wileyonlinelibrary.com]

Rapid Communications in Mass Spectrometry

for $\delta^{18}O$ and $\delta^{2}H$ values has previously been reported for soil and plant extracts analyzed with the L1102-*i* and the L2120-*i* instruments.[4,6,7,9,11,20] The tendency for errors in the L2130-*i* measurements to be positive for $\delta^{18}O$ and $\delta^{2}H$ values has also previously been reported for soil and plant extracts analyzed with the L2130-*i*.[12] These patterns result from the interaction of three factors: (i) the different spectral features that these instruments use to measure the water isotopes (i.e., around 7184 versus 7200 cm^{-1}, respectively), (ii) the differential effects of certain contaminants on those spectral features, and (iii) the abundance of those contaminants in the samples.

A number of compounds are known to produce spectral interference with the water vapor features in the target spectral regions, particularly alcohols and methane.[21] While methane interference can be important for atmospheric measurements, methanol and ethanol tend to be more important for soil and plant measurements. Methanol and ethanol are ubiquitous metabolic intermediates in living plants and microorganisms, and are also produced within dead organic matter through abiotic as well as biotic mechanisms.[22,23] In the water vapor feature around 7184 cm^{-1}, absorption features associated with methanol and ethanol differentially affect the amplitudes of the target $^{1}H^{1}H^{16}O$, $^{1}H^{1}H^{18}O$, and $^{1}H^{2}H^{16}O$ absorption lines, with the result that water samples appear to be depleted in ^{18}O and ^{2}H when either alcohol is present.[3,9] In the water vapor feature around 7200 cm^{-1}, the absorption features associated with methanol and ethanol also differentially affect the amplitudes of the target $^{1}H^{1}H^{16}O$, $^{1}H^{1}H^{18}O$, and $^{1}H^{2}H^{16}O$ absorption lines. However, in this instrument water samples appear to be enriched in ^{18}O and ^{2}H when methanol is present and depleted in ^{18}O and ^{2}H when ethanol is present.[5,10] In combination, these considerations lead us to conclude that methanol was the primary spectral contaminant in the sample set used in this study.

The strong correlations between the CRDS errors and spectral parameters provide a second line of evidence that spectral interference is responsible for the major component of the CRDS errors (Figs. 4–6). In the L2120-*i* measurements, the fact that the 'organic_MeOHampl' parameter was so strongly associated with the isotopic errors supports the interpretation that methanol was the primary spectral contaminant in the distillates (Fig. 4). Given that methanol is not incorporated into the spectral model used in the L2130-*i*, and that the 'residuals' parameter from the L2130-*i* measurements of distillates was linearly associated with the 'organic_MeOHampl' parameter from the L2120-*i* measurements, it appears that either residual methanol or a product of incomplete oxidation of methanol is responsible for the majority of the errors in the L2130-*i* measurements of distillates (Figs. 5 and 7(A)). Previous studies of the MCM have indicated that the effectiveness of the MCM declines continuously as methanol contamination increases, and that the mode of failure appears to be partial conversion of MeOH into CO_2, rather than formation of alternative oxidation products.[9,10] Therefore, the majority of the errors in both the L2120-*i* and the L2130-*i* measurements of distillates in this study seem likely to be attributable to spectral interference from methanol. The few outliers from the methanol error modes are the *Pseudotsuga menziesiii* stem samples (Figs. 5(B)–(D), 5(G)–(I)). The biased baseline parameters for these samples are probably attributable to spectral interference from compounds that have weaker, broader absorbance features than methanol, such as ethanol.[5,6]

In the L2130-*i* measurements of solids, the basis of the errors appears to be more complex. Compared with the L2130-*i* measurements of the stem and leaf distillates, the corresponding measurements of solids were associated with approximately two-fold higher values for the isotopic errors and two-fold wider ranges for the spectral parameters (Fig. 6). This relationship indicates that the overall level of spectral interference for stem and leaf samples was higher for IM extractions than for CVD extractions. In principle, a higher level of spectral interference in the IM extractions could have simply been due to a greater volatilization of methanol in those extractions. However, if this had been the only contributing mechanism, the relationships between the isotopic errors and the spectral parameters would have been invariant for the distillates versus the solids. This was not the case: there was a marked increase in the total noise associated with the solid samples, and the increase in noise was greatest in the samples with the lowest quality spectral fits (Fig. 5 vs Fig. 6). In combination, these relationships suggest that, in addition to methanol, one or more other compounds were generating spectral interference in the IM-CRDS measurements.

There are three differences between the cryogenic extractions and the induction extractions that could lead to extraction of different interfering species: (i) the cryogenic extractions occurred at approximately 10 millitorr, whereas the induction extractions occurred at atmospheric pressure; (ii) the cryogenic extractions were designed to occur at a temperature of approximately 100°C, whereas the induction extractions were designed to occur at temperatures of 180–200°C; and (iii) the distillates from the cryogenic extractions were stored in the liquid phase for several weeks prior to analysis, whereas the vapors from the induction extractions were analyzed in the gas phase within less than a minute of extraction. Of these three factors, the only one that has previously been studied in the context of its effects on water extraction is temperature. In tests with leaf samples, higher extraction temperatures have been found to have species-specific effects, leading to increases in spectral contamination for some species, and decreases for others.[7] In general, this type of mechanism might explain the extraction of different combinations of compounds during the two types of extractions in our study. However, we did not monitor the temperature of the CVD or IM extractions during the experiment, so we cannot quantify the temperatures that the various sets of samples actually experienced.

Non-spectral mechanisms

In several recent studies, it has been proposed that significant components of the isotopic errors in IM-CRDS may be attributable to processes other than spectral interference (i.e., corresponding to mechanisms in classes 1–3 in Table 2). For example, one study has pointed out that the induction module is likely to yield apparent errors when small subsamples are taken from a material where the isotopic composition of water is spatially heterogeneous.[12] A second has pointed out that using the micro-combustion module on

samples with high alcohol content is likely to lead to systematic errors related to the addition of combustion-derived water vapor carrying the ^{18}O-enriched composition of air.[9] A third has suggested that although induction heating appears to retrieve the vast majority of the liquid water from solid samples, this extraction technique may nonetheless produce some sort of substantial non-spectral error due to an unknown mechanism.[11]

In the current study, the only clear evidence that we find for non-spectral errors in any of the CRDS analyses comes from the solid soil samples (Fig. 6). These samples had substantial isotopic errors that had a mean close to zero and were not correlated with any of the spectral parameters, a pattern that is most consistent with variable subsampling of an isotopically heterogeneous matrix (i.e., class 1 in Table 2). In contrast, we find no evidence of systematic errors related to incomplete extraction of matrix-bound water (i.e., class 2 in Table 2), or to the addition of combustion-derived water vapor carrying the ^{18}O-enriched isotopic composition of air (i.e., class 3 in Table 2), or to any other undefined mechanisms. The absence of errors attributable to incomplete extraction of matrix-bound water is probably because the IM extraction protocols were optimized in advance of the experiment in order to achieve complete extractions for each sample type (i.e., see Fig. 2). The absence of errors attributable to combustion-derived water vapor is probably because the manual activated carbon treatment and the in-line activated carbon cartridge were both effective at removing ethanol before samples reached the heated catalyst.

Approaches for correcting errors in CRDS methods

The observations (i) that the isotope errors in the CRDS results are primarily the result of spectral interference and (ii) that spectral interference is a function of the identity and abundance of the interfering compound(s) raise the question of the type of post-processing procedure needed to correct spectrally contaminated isotope measurements. In principle, if several samples differing in water isotopic composition were each contaminated by exactly the same amount(s) of the same interfering compound(s), the absolute value for each sample would be inaccurate, but the relative differences between samples would still be accurate because the errors would be consistent. In this situation, a simple offset correction would be sufficient to correct for the effects of spectral interference. In practice, however, our study illustrates that samples can exhibit substantial variation in the amounts as well as some variation in the identities of the interfering compounds, such that both the absolute values of each sample and the relative differences between samples can be inaccurate. In this situation, approaches that take into account both the identities and the amounts of the interfering compounds are needed to correct for the effects of spectral interference.

For the L2120-*i* measurements of distillates, the post-processing correction based on the organic-filtered amplitudes of the $^{1}H^{1}H^{18}O$, $^{1}H^{1}H^{16}O$, and $^{1}H^{2}H^{16}O$ peaks was highly effective at correcting spectral interference (Figs. 8(A) and 8(D)). The intercepts and slopes that we calculated for regressions between the corrected CRDS values and the IRMS values are nearly identical to those reported for an independent set of samples that were measured on a different L2120-*i* analyzer but corrected analogously.[9] The slight positive bias of the corrected CRDS measurements in the two studies could be the result of the additive effect of laboratory uncertainties and potential sample alteration during transport and storage, as proposed previously,[9] or of a small but systematic bias in the spectral algorithm used to compute the organic-filtered peak amplitudes. Therefore, we concur with the earlier assessment[9] that the post-processing correction based on the organic-filtered peak amplitudes is indeed promising, and that further tests of its accuracy are also warranted.

For the L2130-*i* measurements of distillates and solids, the post-processing corrections based on the 'residuals' parameter were highly and moderately effective, respectively (Figs. 8(B) and 8(C), 8(E) and 8(F)). Since these corrections utilized regression coefficients determined from our specific sample set, it is unclear how successfully they might perform on independent sets of measurements. However, if the dominant error mode in the L2130-*i* measurements is indeed spectral interference from methanol, the path forward is clear. The first step is to revise the L2130-*i* spectral fitting model to include calculation of the component of absorbance due to methanol, as well as the organic-filtered peak amplitudes, as is already done for the L2120-*i*. The second step is to identify the additional species that generate spectral interference when solid samples are extracted with the induction module, and then to develop an appropriate hardware and/or software remedy.

Additional considerations: capital costs, operating costs, and speed

The techniques compared in this study differ not only in accuracy, but also in capital costs, operating costs, and speed. The capital costs of CRDS systems with either the vaporizer and autosampler or the induction module are of the order of $100k, whereas those of IRMS systems with peripherals for water isotope analysis are of the order of $180–250k. Conceptually, the capital costs should be prorated over the lifetime of the instruments. However, because the CRDS systems are relatively new, it is not yet clear how their lifetimes compare with those of IRMS systems. In terms of speed and operating costs, the maximum throughput rate for CVD and manual activated carbon treatment was 80 samples per week. Taking into account the costs of labor and consumables, CVD averaged $7 per sample. When CVD was used to generate liquid extracts for IRMS, the throughput remained limited by CVD and the total costs averaged $43 per sample. When CVD was used with CRDS alone, the throughput also remained limited by the speed of CVD, but the total cost averaged $8 per sample. When CVD was used with IM-CRDS, the throughput decreased to 40 samples per week, and the total costs averaged $28 per sample. When solid samples were directly analyzed via IM-CRDS, the throughput was also 40 samples per week, and the total costs averaged $21 per sample. The reduced throughput of the IM-CRDS analyses was due partially to the need to manually load samples into the IM, and partially to the number of analytical replicates needed to obtain consistent results for samples with high levels of organic contamination.

Rapid Communications in Mass Spectrometry

CONCLUSIONS

The IM-CRDS technique has the potential to provide accurate measurements of the isotopic composition of water in soil, stem, and leaf samples under the following conditions: (i) the isotopic composition of the water in the solid samples is spatially homogeneous relative to the scale of sampling, (ii) the heating parameters in the induction module protocol are optimized to achieve complete extraction of liquid water from the solid sample matrix, (iii) the activated carbon filter reduces the total amount of co-extracted volatile organic compounds to a level that does not overwhelm the oxidation capacity of the heated catalyst; (iv) the heated catalyst produces a complete oxidation of the remaining organic compounds to CO_2 and H_2O; and (v) the total amount of completely oxidized organic compounds is low enough that the nascent water from oxidation does not detectably contaminate the $\delta^{18}O$ value of the sample. If these conditions are satisfied, IM-CRDS can provide isotopic analysis of small samples with similar accuracy, higher speed, and lower cost to CVD and IRMS. However, there are currently many types of water samples that do not satisfy these conditions, and for which IM-CRDS analysis consequently yields variably inaccurate results. The variable accuracy leads to a need for high analytical replication, which both reduces the overall speed and increases the overall cost of IM-CRDS.

Given (i) that the magnitude of the IM-CRDS errors observed in this study is similar to the magnitude of the ecological signals that are of interest in many natural abundance studies and (ii) that spectral interference is the dominant error mode, our interpretation is that measurements from existing IM-CRDS systems can only be considered to be robust if they are subject to spectral analysis and validation. For users who are applying existing IM-CRDS systems to natural abundance measurements, we recommend the following precautions: (i) always include a set of calibration standards delivered on glass fiber filters regardless of the matrix type of the unknowns; (ii) perform calibration experiments to identify threshold values of the diagnostic spectral parameters that delineate acceptable versus unacceptable isotopic errors for particular applications and sample types; (iii) integrate screening of the diagnostic spectral parameters into routine laboratory QA/QC procedures; (iv) discard any analyses where the level of spectral interference results in isotopic errors that exceed the bias thresholds; and (v) cross-check a subset of the analyses that appear to be within the maximum acceptable bias thresholds against CVD and IRMS. Overall, these recommendations are very similar to those previously advocated for other forms of CRDS analysis.[4–7,9] However, implementing spectral screening procedures for IM-CRDS does require the additional step to correct the spectral parameters for the effects of water concentration.[11]

In terms of future development efforts, the current combustion-based version of the IM has already fully overcome the problems related to isotope fractionation that were associated with the original pyrolysis-based version of the device.[24] The primary remaining challenge is resolution of the problems resulting from spectral interference. Towards this end, there are two or three steps with the potential to substantially improve the accuracy of IM-CRDS: (i) identification of all the compounds that cause spectral interference when solid samples are extracted, and either (ii) modification of the combustion step to completely oxidize these compounds to CO_2, and/or (iii) incorporation of corrections for the absorbance associated with these compounds into the spectral fitting models used by the CRDS analyzers to calculate the absorbance of the water isotopologue peaks. Identification of the interfering species is likely to be challenging because there is not yet a comprehensive spectral library that has high-resolution reference spectra in the wavelength regions targeted by the laser-based analyzers. However, if spectral interference can be successfully eliminated, IM-CRDS will have the potential to offer accuracy that is equal to or greater than that of CVD and IRMS. Improved accuracy would probably reduce the need for high levels of analytical replication, translating into increases in the speed and cost-effectiveness of IM-CRDS. The development of an automated sample loader and a sensor to monitor extraction temperatures would also be beneficial. With these types of improvements, IM-CRDS could offer unique advantages for the analysis of the isotopic composition of small samples of matrix-bound water.

Acknowledgements

We are grateful to E. Wright (U. of Arizona), C. Amling (U. of Arizona), and C. C. Amling (U. of Arizona) for assistance designing and constructing the CVD line; to F. Dominguez (U. of Illinois), C. Eastoe (U. of Arizona), and K. Welten (U. of California-Berkeley) for assistance obtaining and calibrating liquid standards; to J. A. Berry (Carnegie Institution) and C. B. Field (Carnegie Institution) for lending the Picarro L2120-*i*; and to J. van Haren (U. of Arizona) for lending the Picarro V1102-*i*. We are also grateful to A. Luketich, N. Power, S. J. Harders, and A. Schaller (U. of Arizona) for assistance performing the IM-CRDS analyses, to C. Douthitt (Thermo Fisher Scientific) for assistance with the cost comparison, and to two anonymous reviewers for suggestions that improved the manuscript. This study was completed with support from the National Science Foundation through the Division of Earth Sciences Award #1255013 (S.A.P.), Macrosystem Biology Program Award #1065790 (R.K.M.), and Major Research Infrastructure Program Award #1040106 (C.B.F. and J.A.B.).

REFERENCES

[1] M. Gehre, H. Geilmann, J. Richter, R. A. Werner, W. A. Brand. Continuous flow $^2H/^1H$ and $^{18}O/^{16}O$ analysis of water samples with dual inlet precision. *Rapid Commun. Mass Spectrom.* **2004**, *18*, 2650.

[2] A. G. West, S. J. Patrickson, J. R. Ehleringer. Water extraction times for plant and soil materials used in stable isotope analysis. *Rapid Commun. Mass Spectrom.* **2006**, *20*, 1317.

[3] W. A. Brand, H. Geilmann, E. R. Crosson, C. W. Rella. Cavity ring-down spectroscopy versus high-temperature conversion isotope ratio mass spectrometry; a case study on δ^2H and $\delta^{18}O$ of pure water samples and alcohol/water mixtures. *Rapid Commun. Mass Spectrom.* **2009**, *23*, 1879.

[4] A. G. West, G. R. Goldsmith, P. D. Brooks, T. E. Dawson. Discrepancies between isotope ratio infrared spectroscopy and isotope ratio mass spectrometry for the stable isotope analysis of plant and soil waters. *Rapid Commun. Mass Spectrom.* **2010**, *24*, 1948.

[5] N. M. Schultz, T. J. Griffis, X. Lee, J. M. Baker. Identification and correction of spectral contamination in $^{2}H/^{1}H$ and $^{18}O/^{16}O$ measured in leaf, stem, and soil water. *Rapid Commun. Mass Spectrom.* **2011**, *25*, 3360.
[6] A. G. West, G. R. Goldsmith, I. Matimati, T. E. Dawson. Spectral analysis software improves confidence in plant and soil water stable isotope analyses performed by isotope ratio infrared spectroscopy (IRIS). *Rapid Commun. Mass Spectrom.* **2011**, *25*, 2268.
[7] M. Schmidt, K. Maseyk, C. Lett, P. Biron, P. Richard, T. Bariac, U. Seibt. Reducing and correcting for contamination of ecosystem water stable isotopes measured by isotope ratio infrared spectroscopy. *Rapid Commun. Mass Spectrom.* **2012**, *26*, 141.
[8] M. Berkelhammer, J. Hu, A. Bailey, D. Noone, C. J. Still, H. Barnard, D. Gochis, G. Hsiao, T. Rahn, A. Turnipseed. The nocturnal water cycle in an open-canopy forest. *J. Geophys. Res. D: Atmos.* **2013**, *118*, 10225.
[9] P. Martín-Gómez, A. Barbeta, J. Voltas, J. Penuelas, K. Dennis, S. Palacio, T. E. Dawson, J. P. Ferrio. Isotope-ratio infrared spectroscopy: a reliable tool for the investigation of plant-water sources? *New Phytol.* **2015**, *207*, 914.
[10] E. Chang, A. Wolf, C. Gerlein-Safdi, K. K. Caylor. Improved removal of volatile organic compounds for laser-based spectroscopy of water isotopes. *Rapid Commun. Mass Spectrom.* **2016**, *30*, 784.
[11] B. E. Lazarus, M. J. Germino, J. L. Vander Veen. Online induction heating for determination of isotope composition of woody stem water with laser spectrometry: a methods assessment. *Isot. Environ. Health Stud.* **2016**, *52*, 309.
[12] N. C. Munksgaard, A. W. Cheesman, C. M. Wurster, L. A. Cernusak, M. I. Bird. Microwave extraction-isotope ratio infrared spectroscopy (ME-IRIS): a novel technique for rapid extraction and in-line analysis of $\delta^{18}O$ and $\delta^{2}H$ values of water in plants, soils and insects. *Rapid Commun. Mass Spectrom.* **2014**, *28*, 2151.
[13] J. Tennyson, P. F. Bernath, L. R. Brown, A. Campargue, M. R. Carleer, A. G. Császár, R. R. Gamache, J. T. Hodges, A. Jenouvrier, O. V. Naumenko, O. L. Polyansky, L. S. Rothman, R. A. Toth, A. C. Vandaele, *et al*. IUPAC critical evaluation of the rotational–vibrational spectra of water vapor. Part I – Energy levels and transition wavenumbers for $H_2^{17}O$ and $H_2^{18}O$. *J. Quant. Spectrosc. Radiat. Transfer* **2009**, *110*, 573.
[14] J. Tennyson, P. F. Bernath, L. R. Brown, A. Campargue, A. G. Császár, L. Daumont, R. R. Gamache, J. T. Hodges, O. V. Naumenko, O. L. Polyansky, L. S. Rothman, R. A. Toth, A. C. Vandaele, N. F. Zobov, *et al*. IUPAC critical evaluation of the rotational–vibrational spectra of water vapor. Part II – Energy levels and transition wavenumbers for $HD^{16}O$, $HD^{17}O$, and $HD^{18}O$. *J. Quant. Spectrosc. Radiat. Transfer* **2010**, *111*, 2160.
[15] J. Tennyson, P. F. Bernath, L. R. Brown, A. Campargue, A. G. Császár, L. Daumont, R. R. Gamache, J. T. Hodges, O. V. Naumenko, O. L. Polyansky, L. S. Rothman, A. C. Vandaele, N. F. Zobov, A. R. Al Derzi, *et al*. IUPAC critical evaluation of the rotational–vibrational spectra of water vapor, Part III – Energy levels and transition wavenumbers for $H_2^{16}O$. *J. Quant. Spectrosc. Radiat. Transfer* **2013**, *117*, 29.
[16] R Core Team. *R: A language and environment for statistical computing*. R Foundation for Statistical Computing, Vienna, Austria, **2016**. http://www.R-project.org/.
[17] D. Bates, M. Maechler, B. Bolker, S. Walker. Fitting linear mixed-effects models using lme4. *J. Statist. Software* **2015**, *67*, 1.
[18] A. Kuznetsova, P. B. Brockhoff, R. H. B. Christensen. lmerTest: Tests in linear mixed effects models. R package version 2.0-32, **2016**. https://CRAN.R-project.org/package=lmerTest.
[19] S. Nakagawa, H. Schielzeth. A general and simple method for obtaining R^2 from generalized linear mixed-effects models. *Methods Ecol. Evol.* **2013**, *4*, 133.
[20] L. Zhao, H. Xiao, J. Zhou, L. Wang, G. Cheng, M. Zhou, L. Yin, M. F. McCabe. Detailed assessment of isotope ratio infrared spectroscopy and isotope ratio mass spectrometry for the stable isotope analysis of plant and soil waters. *Rapid Commun. Mass Spectrom.* **2011**, *25*, 3071.
[21] M. J. Hendry, B. Richman, L. I. Wassenaar. Correcting for methane interferences on $\delta^{2}H$ and $\delta^{18}O$ measurements in pore water using $H_2O_{(liquid)}$–$H_2O_{(vapor)}$ equilibration laser spectroscopy. *Anal. Chem.* **2011**, *83*, 5789.
[22] C. Warneke, T. Karl, H. Judmaier, A. Hansel, A. Jordan, W. Lindinger, P. Crutzen. Acetone, methanol, and other partially oxidized volatile organic emissions from dead plant matter by abiological processes: Significance for atmospheric HO_x chemistry. *Global Biogeochem. Cycles* **1999**, *13*, 9.
[23] C. M. Gray, R. K. Monson, N. Fierer. Emissions of volatile organic compounds during the decomposition of plant litter. *J. Geophys. Res.* **2010**, *115*, G03015.
[24] N. Saad, G. Hsiao, L. Chapellet-Volpini, D. Vu. Two-pronged approach to overcome spectroscopically interfering organic compounds with isotopic water analysis. EGU General Assembly Conference Abstracts, **2013**.

SUPPORTING INFORMATION

Additional supporting information may be found in the online version of this article at the publisher's website.

